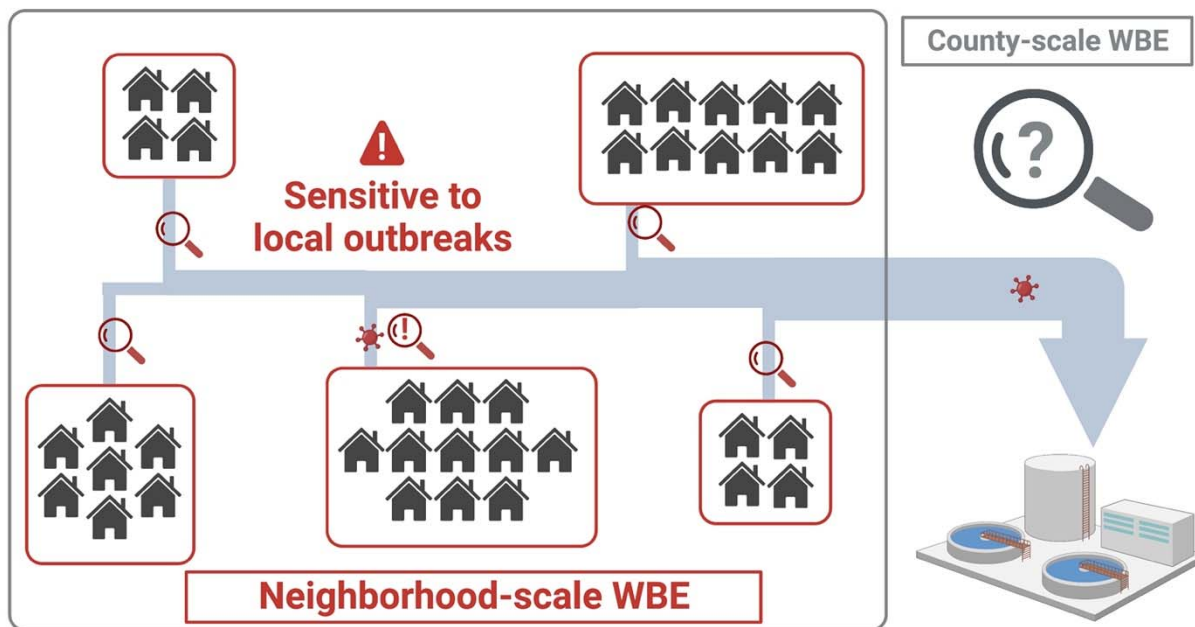


24

25

Graphical abstract



26

27

28

29
30
31
32
33
34
35
36
37
38
39
40
41
42
43
44
45
46
47
48

Abstract

Wastewater-based epidemiology (WBE), an emerging approach for community-wide COVID-19 surveillance, was primarily characterized at large sewersheds such as wastewater treatment plants serving a large population. Although informed public health measures can be better implemented for a small population, WBE for neighborhood-scale sewersheds is less studied and not fully understood. This study applied WBE to seven neighborhood-scale sewersheds (average population of 1,471) from January to November, 2021. Community testing data showed an average of 0.004% incidence rate in these sewersheds (97% of monitoring periods reported two or fewer daily infections). In 92% of sewage samples, SARS-CoV-2 N gene fragments were below the limit of quantification. We statistically determined $10^{-2.6}$ as the threshold of the SARS-CoV-2 N gene concentration normalized to pepper mild mottle virus (N/PMMOV) to alert high COVID-19 incidence rate in the studied sewershed. This threshold of N/PMMOV identified neighborhood-scale outbreaks (COVID-19 incidence rate higher than 0.2%) with 82% sensitivity and 51% specificity. Importantly, neighborhood-scale WBE can discern local outbreaks that would not otherwise be identified by city-scale WBE. Our findings suggest that neighborhood-scale WBE is an effective community-wide disease surveillance tool when COVID-19 incidence is maintained at a low level.

Keywords: Wastewater-based epidemiology; neighborhood-scale sewersheds; SARS-CoV-2 variant-specific RT-qPCR assays; low COVID-19 incidence.

49 **Introduction**

50 Wastewater-based epidemiology (WBE) has been used as a cost-effective epidemiological tool
51 for community-wide COVID-19 surveillance worldwide (Chen et al., 2020; Hart and Halden,
52 2020; Sherchan et al., 2021; Tiwari et al., 2021). For example, WBE has been shown to be able
53 to detect SARS-CoV-2 at an 0.01% incidence (1 infection in 10,000 people) when the influence
54 of wastewater treatment plants serving a community of more than 100,000 residents was
55 analyzed (Hata et al., 2021). In addition, the viral genome concentrations in sewersheds may be a
56 better proxy for actual disease incidence than the reported COVID-19 infection cases because
57 reported cases are significantly affected by temporal clinical testing capacity (Xiao et al., 2022).
58 Furthermore, WBE allows for longitudinal wastewater surveillance to predict disease outbreaks
59 in advance of clinical epidemiology because SARS-CoV-2 genes are shed before symptom onset
60 (Wu et al., 2022b).

61 Large-scale sewersheds (such as wastewater treatment plants serving hundreds of
62 thousands to millions of people) have routinely been surveilled for COVID-19 since early 2020
63 (Hata et al., 2021; Xiao et al., 2022). However, the large-sized sewersheds may not provide
64 detailed information for region-specific public health measures. For example, social determinants
65 of COVID-19 risk, such as demographics and socioeconomic status, which are regional
66 characteristics (Abrams and Szeffler, 2020; Jamal et al., 2022; Upshaw et al., 2021), may not be
67 reflected in the influent wastewater from large sewersheds. The heterogeneity of these social
68 determinants across the sewersheds is a possible explanation for discrepancies between state-
69 wide and county-specific COVID-19 data (Messner and Payson, 2020). WBE also has been
70 applied to small-scale sewersheds, such as buildings on university campuses (Bivins and Bibby,
71 2021; Gibas et al., 2021; Karthikeyan et al., 2021). At this smaller scale, viruses are detected in

72 wastewater when there are COVID-19 infection cases in the buildings. However, building-scale
73 monitoring is not practical for residential areas with high numbers of single-family homes.

74 Neighborhood-scale monitoring for COVID-19 has been conducted (Barrios et al., 2021;
75 Spurbeck et al., 2021). While this neighborhood-scale monitoring could allow for a more
76 targeted public health intervention in a specific community, SARS-CoV-2 N gene concentrations
77 presented lower correlation coefficients with COVID-19 infection cases as the catchment
78 populations decreased (Bitter et al., 2022; Rusiñol et al., 2021; Sangsanont et al., 2022).
79 Additionally, the probability of SARS-CoV-2 detection in wastewater samples at a given
80 COVID-19 incidence decreases with a decrease in the population size (Fitzgerald et al., 2021;
81 Wu et al., 2021). Thus, neighborhood scale monitoring strategies are a possible area of
82 improvement.

83 This study aims to develop a methodology for the neighborhood-scale WBE for
84 community-wide COVID-19 surveillance. We collected sewage samples from seven
85 neighborhood-scale sewersheds (average population of 1,471 people) across Champaign County,
86 IL, USA for eleven months. First, we analyzed the SARS-CoV-2 N gene, S:A570D mutation,
87 and S:P681R mutation. These two mutations are confirmed by in silico analysis and in vitro
88 experiments to be exclusive to the Alpha and Delta variants circulating in IL, USA, during our
89 monitoring period (Oh et al., 2022b). Then, we plotted these data onto the clinical COVID-19
90 testing data obtained from the neighborhood-scale sewersheds, allowing us to estimate high
91 COVID-19 incidence with WBE data. Our data uncovered local outbreaks that county-scale
92 WBE would not detect and the introduction of SARS-CoV-2 variants of concern to the
93 sewersheds even at low COVID-19 incidence. Our findings suggest that the neighborhood scale
94 WBE will contribute to COVID-19 surveillance, especially when COVID-19 incidence is low.

95

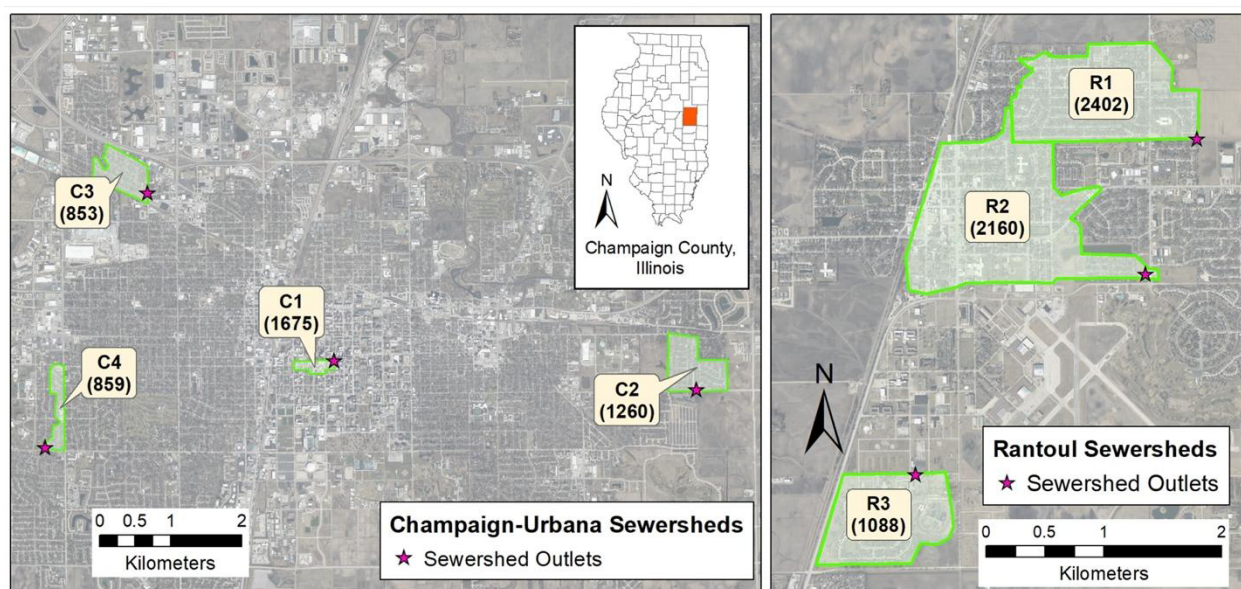
96 **Materials and Methods**

97 **Collection of raw sewage composite samples**

98 We selected eleven sampling points of manholes across Champaign County, IL, USA. Among
99 these, four sampling points (C1, C2, C3, and C4) receive sewage discharged from Champaign
100 and Urbana cities, and three sampling points (R1, R2, and R3) receive sewage discharged
101 Rantoul town. The areas of these seven neighborhood-scale sewersheds vary from 0.09 to 1.70
102 km². The populations in these sewersheds ranged from 853 to 2402 in 2020 (**Fig. 1**). We
103 monitored these seven sewersheds (C1, C2, C3, C4, R1, R2, and R3) from January 2021 to
104 November 2021, during which we collected 254 sewage samples in total. We also collected
105 wastewater from a food processing plant. The amount of human fecal matter released in this
106 wastewater is much smaller than the processing water from slaughtering and meatpacking. For
107 this reason, we used this wastewater for process control, evaluating cross-contamination among
108 the sewage samples during the sample processing.

109 In 2022, we chose another three sampling points in rural areas of Champaign County (S1,
110 S2, and S3), which were less accessible to clinical testing, to supplement community-wide
111 COVID-19 surveillance. Because the sanitary sewer was not connected to most houses in these
112 areas (S1, S2, and S3 served populations of 9094, 3547, and 5547 people, respectively), we
113 collected sewage from local schools that could represent COVID-19 incidence in these areas. It
114 has been shown recently that surveillance at school gave insight into community transmission
115 (Castro-Gutierrez et al., 2022). We also examined wastewater from the Urbana-Champaign
116 Sanitary District (IL, USA), serving 144,097 people living in the cities of Champaign and
117 Urbana and adjacent areas. Although there were two city-scale wastewater treatment plants in

118 this district, we collected wastewater from one of these two plants (City) with the assumption
119 that each wastewater treatment plant represents the entire sewershed. We analyzed 44 samples
120 from the four sewersheds (S1, S2, S3, and City) from January 2022 to March 2022.
121



122
123 **Fig. 1.** Map of sewersheds in (A) Champaign and Urbana cities and (B) Rantoul town in Illinois.
124 Values in parenthesis are population estimates using block-level US Census 2020 data.
125

126 We installed autosamplers (Teledyne ISCO, USA) programmed to collect a 1 to 2 L
127 composite sample of sewage pumped at 4-hour intervals for four days. First, the composite
128 samples were transferred to sterile sampling bags (14-955-001, Fisher Scientific, USA), and 20
129 mL of 2.5 M $MgCl_2$ was added to the samples (i.e., final $MgCl_2$ concentrations from 25 to 50
130 mM) to coagulate solids including virus particles (Ahmed et al., 2020b; Oh et al., 2022a). Next,
131 samples were transported on ice to a laboratory at the University of Illinois Urbana-Champaign
132 within three hours. All contact material was sanitized with 10% bleach and 70% ethanol to
133 minimize cross-contamination whenever handling different samples. The minimum
134 recommended meta-information on sewage samples is summarized in **Table S1**.

135

136 **Sample processing and viral nucleic acid extraction**

137 Upon arrival at the laboratory, supernatants from each composite sample were discarded. The
138 remaining 35 mL of sewage, in which solid particles were concentrated, were transferred to a 50
139 mL tube (12-565-271, Fisher Scientific, USA). Next, we added 350 μ L of 10^5 gene copies
140 (gc)/ μ L of bovine coronavirus (BCoV; 16445-1, Merck Animal Health, USA) to the 35 mL of
141 concentrated sewage. After a 10 minutes incubation at room temperature, samples were
142 centrifuged at 10,000 g for 30 minutes (Sorvall™ RC 6 Plus, Thermo Scientific, USA).
143 Supernatants were then discarded and a portion of the concentrated sludge (100 μ L) was
144 transferred to a sterile 1.5 mL tube (1415-2600, USA Scientific, USA). Total RNA and DNA,
145 including SARS-CoV-2 RNA, were extracted from the sludge with QIAamp Viral RNA mini kit
146 (Qiagen, German) following the manufacturer's procedure with a minor modification. The final
147 volume of extracts was 100 μ L. Sewage collection and processing were conducted on the same
148 day, and the RNA samples were stored at -80 °C until downstream analysis.

149

150 **Analysis of viral genomes**

151 Total RNA was diluted serially 10-fold, and six reverse transcriptase quantitative polymerase
152 chain reaction (RT-qPCR) assays (**Table S2**) were used to analyze samples for the presence of
153 SARS-CoV-2 RNA. We quantified the N gene (i.e., N1 assay with 2019-nCoV RUO kit,
154 Integrated DNA Technologies, USA) to identify a total SARS-CoV-2 RNA concentration. We
155 also analyzed samples for the presence of the S:A570D and S:P681R mutations in the Alpha and
156 Delta variants, as these were dominant variants in our study area during our sample collection
157 (Oh et al., 2022b). For the data quality assurance, we quantified pepper mild mottle virus

158 (PMMOV), Tulane virus (TV), and BCoV, which were used to normalize SARS-CoV-2 to
159 human fecal matter, determine the impact of PCR inhibitors, and calculate SARS-CoV-2
160 recovery efficiency, respectively.

161 The details for RT-qPCR assays are summarized in **Table S3**, following MIQE
162 guidelines (Bustin et al., 2009). We analyzed five targets (i.e., N gene, S:A570D, S:P681R,
163 PMMOV, and TV) by Taqman-based RT-qPCR assays. We designed two duplex RT-qPCR
164 assays and one singleplex RT-qPCR to analyze these five targets. We used the first duplex RT-
165 qPCR assay to detect total SARS-CoV-2 RNA (i.e., N gene) and the S:A570D mutation. The
166 second was used to analyze the S:P681R mutation and PMMoV. To validate the two duplex RT-
167 qPCR assays, we compared C_q values of serial dilutions of synthetic RNA/DNA standard
168 controls determined by duplex RT-qPCR and its corresponding singleplex RT-qPCR. We used
169 singleplex RT-qPCR to measure TV RNA. The Taqman-based RT-qPCR started with mixing 5
170 μ L of RNA sample, 5 μ L of Taqman Fast Virus 1-step Master Mix (4444432, Applied
171 Biosystems, USA), 1 μ L of primers/probe mixture for each assay (i.e., final concentrations of
172 400 nM for primers and 200 nM for probes), and various volumes of nuclease-free water that fill
173 up the mixture to 20 μ L. For example, we added 1 μ L of primer/probe for the N gene, 1 μ L of
174 primer/probe for the S:A570D mutation, and 8 μ L of nuclease-free water to the RT-qPCR
175 cocktail for the first duplex RT-qPCR assay while 1 μ L of primer/probe for TV and 9 μ L of
176 nuclease-free water to the RT-qPCR cocktail for the singleplex RT-qPCR assay. The PCR
177 cocktail was placed in 384-well plates (4309849, Thermofisher Scientific, USA) and analyzed by
178 QuantStudio 7 Flex (Thermofisher, USA) with a thermal cycle of 5 minutes at 50 $^{\circ}$ C, 20 seconds
179 at 95 $^{\circ}$ C followed by 45 cycles of 15 seconds at 95 $^{\circ}$ C and 60 seconds at 60 $^{\circ}$ C. The PCR standard
180 curves were obtained for every RT-qPCR analysis with 10-fold serial dilutions of synthetic RNA

181 or DNA controls, and average PCR efficiencies for RT-qPCR were 92% (**Fig. S1**). Four
182 replicates of nuclease-free water were run for every RT-qPCR analysis to identify the
183 contamination of reagents or cross-contamination among reactions. These non-template controls
184 tested negative in all RT-qPCR analyses represented in our dataset. We also determined the limit
185 of detection (LOD) and limit of quantification (LOQ) for each assay with 20 replicates of serial
186 dilutions of synthetic controls (**Table S4, S5, and S6**), following a previous study (Oh et al.,
187 2022b).

188 We analyzed BCoV RNA by a SYBR-based RT-qPCR assay. The RT-qPCR mixture for
189 SYBR-based RT-qPCR assay included 3 μL of RNA sample, 0.3 μL of 10 μM forward and
190 reverse primer, 1.275 μL of molecular biology grade water (Corning, NY, USA), 5 μL of 2 \times iTaq
191 universal SYBR green reaction mix, 0.125 μL of iScript reverse transcriptase from the iTaqTM
192 Universal SYBR[®] Green One-Step Kit (1725151, Bio-Rad Laboratories, USA). The PCR
193 cocktail was placed in 96-well plates (4306737, Applied Biosystems, USA) and analyzed by an
194 RT-qPCR system (QuantStudio 3, Thermo Fisher Scientific, USA). The RT-qPCR reaction was
195 performed with a thermocycle of 50 $^{\circ}\text{C}$ for 10 minutes and 95 $^{\circ}\text{C}$ for 1 minute, followed by 40
196 cycles of 95 $^{\circ}\text{C}$ for 10 seconds and 60 $^{\circ}\text{C}$ for 30 seconds. Melting curves were analyzed while the
197 temperature increased from 60 $^{\circ}\text{C}$ to 95 $^{\circ}\text{C}$. The melting curves showed that the primers were
198 specifically bound to the target genome. The SYBR signal was normalized to the ROX reference
199 dye. The cycles of quantification (Cq) were determined by QuantStudio Design & Analysis
200 Software (v1.5.1). The numbers of technical replicates were 4 for synthetic RNA controls and
201 from 3 to 5 for sewage samples. The PCR efficiencies for RT-qPCR were higher than 85%
202 ($R^2 > 0.99$).

203 Once RNA concentrations in the final extracts were determined, we calculated RNA
204 concentrations in sewage samples using Eqs. 1-4.

205

$$206 \quad C_{sludge} = C_{RNA\ extract} \times \frac{V_{RNA\ extract}}{V_{sludge}} \quad (\text{Eq. 1})$$

$$207 \quad RE = \frac{C_{BCoV\ in\ sludge} \times V_{sludge}}{C_{BCoV\ in\ stock\ solution} \times V_{stock\ solution}} \quad (\text{Eq. 2})$$

$$208 \quad CF = \frac{V_{sludge}}{V_{initial\ sewage}} \quad (\text{Eq. 3})$$

$$209 \quad C_{initial\ sewage} = C_{sludge} \times \frac{CF}{RE} \quad (\text{Eq. 4})$$

210

211 Where $C_{RNA\ extract}$, C_{sludge} , and $C_{initial\ sewage}$ indicate RNA concentration in RNA extract, sludge,
212 and initial sewage, respectively. $V_{RNA\ extract}$, V_{sludge} , and $V_{initial\ solution}$ mean volume of RNA extract,
213 sludge, and initial sewage, respectively. RE and CF represent recovery efficiency and
214 concentration factor, respectively.

215

216 **Testing for PCR inhibitors**

217 We evaluated the impacts of potential remaining PCR inhibitors in the RNA extracts by spiking
218 RNA extracts with TV RNA. TV is a calicivirus that infects rhesus monkeys, so the TV should
219 not be present in our collected sewage samples. We added 1 μL of 10^6 gc/ μL TV RNA to 10 μL
220 RNA extracts and 10 μL molecular biology-grade water (Millipore Sigma, Burlington, MA,
221 USA). We assumed that if an RNA extract included PCR inhibitors, a Cq value for TV in the
222 RNA extract would be higher by 1 Cq value or more than in inhibition-free water.

223

224 **Presentation of viral genome concentrations**

225 If one of the technical replicates for RT-qPCR is undetermined until 45 PCR cycles, then viral
226 genome concentrations are not quantitatively reliable (Safford et al., 2022; **Fig. S2A**). Hewitt et
227 al. (2022) and **Fig. S2B** showed that positivity/negativity (Eq. 5) is a better indicator for the
228 actual genome concentrations than the C_q values when samples have undetermined RT-qPCR
229 results. We used standard curves to convert C_q values to concentrations when none of the
230 technical RT-qPCR replicates were undetermined. On the other hand, when undetermined data
231 was reported, we used positivity to estimate viral RNA concentrations (Eq. 6).

232

$$233 \quad P_S = \frac{\textit{The number of positive replicates}}{\textit{Total number of replicates}} \quad (\text{Eq. 5})$$

$$234 \quad C_S = C_L \times P_S \quad (\text{Eq. 6})$$

235

236 Where C_S represents the N gene concentration of samples containing undetermined qPCR results
237 in technical replicates. C_L indicates the lowest N gene concentration from samples that do not
238 have undetermined qPCR results. In addition, as suggested in previous studies (Simpson et al.,
239 2021; U.S. CDC, 2022a; Wolfe et al., 2021; Zhan et al., 2022), we presented SARS-CoV-2 RNA
240 concentrations normalized to PMMOV, an indicator for human fecal matter, for comparisons
241 with clinical epidemiology.

242

243 **Using BCoV spiked experiments to determine sample composite period**

244 We put 35 mL of sewage sample and 350 μL of 10⁵ gc/μL BCoV particles in a 50 mL sterile
245 tube. The five tubes of the sewage samples containing BCoV were incubated in a water bath
246 where the temperature was maintained at 25°. We collected samples every 24 hours for five

247 days. The number of BCoV RNA was determined by the extraction method and RT-qPCR assays
248 mentioned above. We assumed that the RNA decay follows the first-order decay model (Eq. 7).

249

$$250 \quad C_t = C_0 e^{-kt} \quad (\text{Eq. 7})$$

$$251 \quad \ln C_t = \ln C_0 - kt \quad (\text{Eq. 8})$$

252

253 Where C_t and C_0 are the concentration of BCoV RNA at time t and zero, k is the first-order
254 decay rate constant. The rate constant is equal to the slope of $\ln C$ and the time graph (Eq. 8),
255 which was determined by the linear least-squares regression model.

256

257 **Clinical epidemiology**

258 The Champaign-Urbana Public Health District (CUPHD) provided daily COVID-19 cases with
259 spatiotemporal information for the eight sewersheds (the Urbana-Champaign Sanitary District
260 (UCSD), C1, C2, C3, C4, R1, R2, and R3). Note that there are two wastewater treatment plants
261 in the UCSD, including the one monitored in this study (i.e., City). We assumed that the
262 incidence rates on the City sewershed were the same as that on the entire UCSD sewershed. With
263 the daily COVID-19 cases, we determined the 7-day average and relative infection case. The
264 relative infection case refers to the number of patients actively contributing to sewage viral load.
265 The relative infection case is determined by multiplying temporal daily COVID-19 cases by a
266 virus shedding model (He et al., 2020; Hewitt et al., 2022). We determined the COVID-19
267 incidence rate for each sewershed by normalizing the COVID-19 occurrence (cases/day) to the
268 corresponding populations.

269

270
$$\text{Incidence rate (\%)} = \frac{\text{COVID-19 occurrence (cases/day)}}{\text{population in a sewershed (people)}} \times 100 \quad (\text{Eq. 9})$$

271
272 The CDC uses a criterion of 200 people or more COVID-19 cases per 100,000 people for 7 days
273 as one of the metrics to issue a warning of the high level of COVID-19 cases (U.S. CDC, 2022b).
274 According to the virus shedding model, one infected case is assumed to shed viruses 3 days
275 before and 9 days after the symptom onset date. The total virus number of one case shed during
276 this active 13 days equals that of 7.06 people shed on the symptom onset date. Thus, the CDC's
277 metric is equivalent to a 0.2% incidence rate (Eq. 9).

278 We analyzed 138 sequences from the Global Initiative on Sharing All Influenza Data
279 (GISAID), which were reported from Champaign County in 2021 using an algorithm, PRIMES
280 developed by Oh et al. (2022b), to determine the temporal prevalence of SARS-CoV-2 variants
281 in Champaign County.

282
283 **Statistical analysis**

284 We conducted various statistical analyses to support the credibility of data comparisons.
285 Specifically, BCoV RNA concentrations in sewage with different incubation times were
286 analyzed by Mann-Whitney U Test and a linear least-squares regression model (**Fig. S3**).
287 PMMOV and BCoV RNA concentrations were not normally distributed, so Kruskal Wallis
288 ANOVA was used to compare these data across the seven sewersheds (**Fig. S4** and **Fig. S5**). The
289 Cq values of serial dilutions determined by multiplex and singleplex RT-qPCR assays were
290 compared by F-tests (**Fig. S7**). In addition, N/PMMOV was not normally distributed, so we used
291 Spearman's rank correlation to compare it to clinical epidemiology (**Table S7**). A receiver
292 operating characteristics (ROC) curve summarizes sensitivity and specificity with a series of

293 N/PMMOV values to indicate COVID-19 incidence rates higher than 0.2%. Sensitivity and
294 specificity were calculated for each N/PMMOV value with Eqs. 10-11.

295

$$296 \text{ Sensitivity} = \frac{\text{True positives}}{\text{True positives} + \text{False negatives}} \quad (\text{Eq. 10})$$

$$297 \text{ Specificity} = \frac{\text{True negatives}}{\text{True negatives} + \text{False positives}} \quad (\text{Eq. 11})$$

298

299 True positives refer to the number of monitoring periods that show high PMMOV and high
300 incidence levels while true negatives refer to the number of monitoring periods showing low
301 PMMOV and incidence levels. False positives indicate the number of monitoring periods that
302 show high PMMOV but low incidence levels while false negatives represent the number of
303 monitoring periods that show low PMMOV but high incidence levels. These statistical analyses
304 were performed using OriginPro (version 2019b). Furthermore, we analyzed the possibility of
305 detecting the SARS-CoV-2 N gene at a given COVID-19 incidence by a binary logistic
306 regression model (**Fig. 5**). This statistical analysis was performed using the *statsmodels* library in
307 Python (version 3.8.8) (Seabold and Josef Perktold, 2010) and the algorithm is deposited at
308 https://github.com/Nguyen205/Logistic_regression.

309

310 **Results and Discussion**

311 **Quality assurance and quality control**

312 We first identified an appropriate sample composite period to establish an efficient WBE
313 procedure by spiking samples with known amounts of bovine coronavirus (BCoV) RNA and
314 examining its stability over time. **Fig. S3** used controlled laboratory conditions and showed the
315 concentrations of BCoV RNA as the incubation time increased. The reduction in BCoV RNA

316 concentrations followed first-order decay kinetics ($R^2=1.00$) with a first-order decay rate
317 constant of 0.22 day^{-1} , which is within the range of previously reported rate constants for SARS-
318 CoV-2 and PMMOV (Roldan-Hernandez et al., 2022). Under these conditions, BCoV RNA
319 concentrations were not significantly different from initial concentrations at four days post-
320 incubation (Mann-Whitney U Test; $p>0.05$). Ahmed et al. (2020a) found similar results when
321 using SARS-CoV-2. The temperatures measured at our sampling sites were lower than 25°C
322 throughout the monitoring period. Therefore, we were assured that coronavirus RNA genomes
323 would remain stable when we collected 4-day composite sewage samples.

324 PMMOV RNA concentrations were quantified for each composite sample as an indicator
325 that fecal material was present in a composite sample (D'Aoust et al., 2021). The PMMOV RNA
326 concentrations for all collected samples across the seven collection sites are different (Kruskal
327 Wallis ANOVA; $p<0.05$, **Fig. S4**). This observation was expected because of the heterogeneity
328 in the sewage composition. Median values of PMMOV RNA concentrations from the seven
329 sewersheds ranged from $10^{6.41}$ (C2) to $10^{7.05}$ gc/L (R1), which were similar to those previously
330 reported (Feng et al., 2021). Since PMMOV was detected from all collected sewage samples, our
331 sampling method successfully contained human fecal matter from sewer distribution systems.

332 We used the recovery efficiency for BCoV to evaluate the sample processing procedures
333 (e.g., sludge concentration and RNA extraction). The mean, median, minimum, and maximum
334 recovery efficiencies across the seven locations were 3.4%, 1.5%, 0.02%, and 64%, respectively.
335 The recovery efficiencies differed significantly (Kruskal Wallis ANOVA; $p<0.05$, **Fig. S5**). A
336 wide range of recovery efficiency was also reported previously (Feng et al., 2021), and the
337 differences were probably attributed to different sewage characteristics. Pecson et al. (2021)
338 investigated the reproducibility and sensitivity of 36 virus concentration methods performed by

339 32 laboratories across the U.S. They suggested a threshold of 0.01% of recovery efficiency for
340 the exclusion of poorly processed samples. Based on this criterion, none of the samples were
341 screened out due to the low quality of sample processing.

342 Sewage samples routinely contain PCR inhibitors (Rački et al., 2014). Thus, it is essential
343 to determine the impact of remaining PCR inhibitors in the final RNA extracts. We conducted
344 experiments to determine the presence of RNA inhibitors by spiking samples with Tulane Virus
345 (TV) RNA. Results are shown in **Fig. S6**. We found that all ΔCq values were within 1.0,
346 confirming that PCR inhibitors' impacts in our RNA samples were negligible after 10-fold
347 dilution.

348 We used multiplex RT-qPCR assays to quantify the SARS-CoV-2 N gene, the S:A570D
349 mutation for the Alpha variant, the S:P681R mutation for the Delta variant, and PMMOV
350 replication gene in the final RNA extracts to save samples, reagents, and time. **Fig. S7** shows that
351 the Cq values from singleplex and multiplex RT-qPCR were not significantly different for the
352 two sets of multiplex RT-qPCR assays (F-test; $p > 0.05$). Thus, the fluorescence from FAM dye
353 did not affect the HEX channel and vice versa. For the final negative control, we applied the
354 same procedures, including sample collection, processing, and analysis, to wastewater
355 discharged from a food processing plant and sewage samples. We did not detect a SARS-CoV-2
356 RNA signal (i.e., Cq values were undetermined by 45 cycles of RT-qPCR) from any of the food
357 processing wastewater samples throughout the monitoring period. This finding suggests no
358 cross-contamination among samples from different sites occurred, so it can be assumed that the
359 positive Cq values were true positives.

360

361 **Comparisons of clinical epidemiology and wastewater-based epidemiology data**

362 WBE has been evaluated based on the goodness of fit to clinical epidemiology determined by
363 statistical models such as a Pearson correlation coefficient or a Spearman rank correlation
364 coefficient (Barua et al., 2022; Li et al., 2021), depending on the data normality. Similarly, we
365 compared N/PMMOV ratios to COVID-19 incidence rates determined by three epidemiological
366 parameters: daily COVID-19 cases (Xiao et al., 2022), 7-day average COVID-19 cases
367 (Catherine Hoar et al., 2022), and relative infection COVID-19 cases (Hewitt et al., 2022). Then,
368 we evaluated the goodness of fit by Spearman rank correlation (**Table S7**) between the
369 N/PMMOV ratios and these epidemiological parameters. We found that the relative infection
370 cases yielded higher correlation coefficients than daily cases and 7-day averages at six
371 sewersheds (C1, C2, C3, C4, R1, and R2). Therefore, we used relative infection cases to
372 determine the COVID-19 incidence rate.

373 The correlation coefficient between COVID-19 incidence rate and N/PMMOV ranged
374 from 0.08 (R3) to 0.72 (C1) across the seven sewersheds (C1, C2, C3, C4, R1, R2, and R3)
375 (**Table S7**). Overall, the correlation coefficients showed a considerable variation among the
376 sewersheds. There are several possible explanations for the lack of uniform correlations.

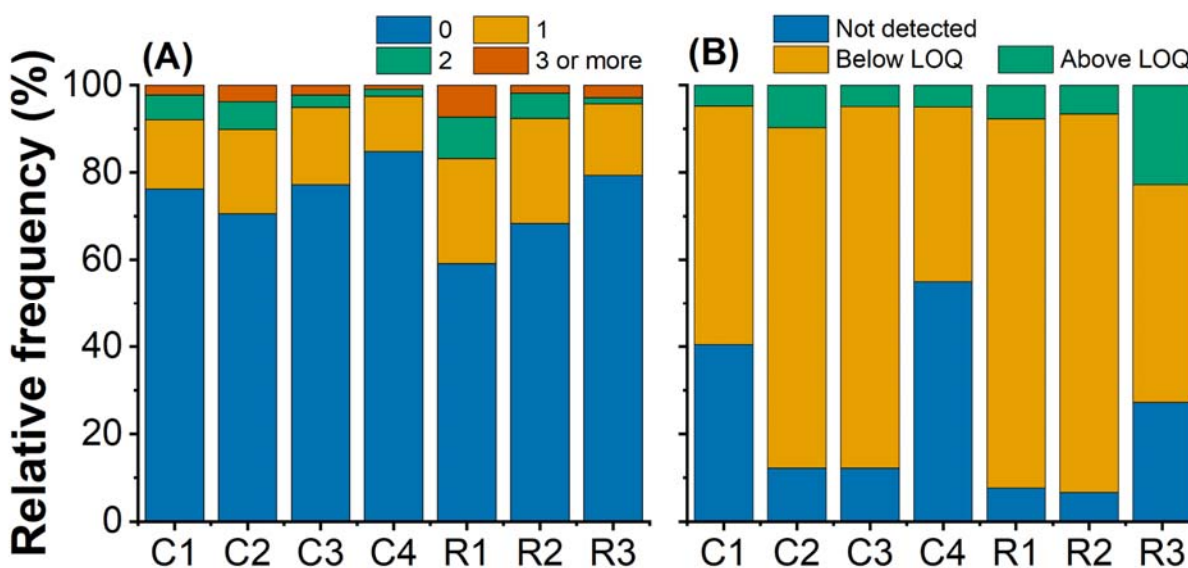
377 First, the average COVID-19 incidence rate was 0.004% throughout the monitoring
378 period, equivalent to only a few daily COVID-19 cases in neighborhood-scale sewersheds
379 serving populations of around 1,400 people. **Fig. 2A** shows that no COVID-19 patients were
380 reported at the seven sewersheds for 221 days out of 301 days of average monitoring periods (i.e.,
381 73.4%). One, two, and three or more patients were reported at 18.7, 4.9, and 3.0%, respectively.
382 Individual patients have significant differences in clinical symptoms, viral shedding, and access
383 to COVID-19 tests. For example, Ke et al. (2022) found substantial person-to-person variations

384 in viral load and virus shedding duration among COVID-19 patients. A time lag between
385 symptom onset and testing date also varies because people in different locations have different
386 access to COVID-19 testing. The fact that the different time lags significantly impact the
387 correlation to the WBE data is demonstrated by the highest correlation coefficient (0.72) at
388 location C1. Most residents of location C1 were undergraduate students enrolled at the
389 University of Illinois Urbana-Champaign, which required students to undergo routine COVID-19
390 testing. For example, graduate students were required to get tested once a week until August
391 2021. Undergraduate students were required to get tested twice a week until May 2021 and once
392 a week from May to August 2021. While the mandatory COVID-19 testing was lifted for fully
393 vaccinated individuals in September 2021, many residents in campus town still got weekly
394 testing. Therefore, compared to other sites, the reported COVID-19 cases at C1 were much
395 closer to the actual infection cases. The individual heterogeneity in clinical symptoms, including
396 virus shedding and access to COVID-19 tests, will become more significant as the number of
397 COVID-19 cases decreases.

398 Second, SARS-CoV-2 RNA was present at a low concentration in sewage samples. The
399 SARS-CoV-2 N gene concentrations are summarized in three groups (**Fig. 2B**); the N gene was
400 not detected; the N gene was detected in at least one of the qPCR replicates, but the
401 concentrations were below LOQ; and the N gene concentrations were above the LOQ. We found
402 that the N gene was detected in 77% of the sewage samples, which agrees with the detection rate
403 of composite wastewater samples determined by meta-analyses (a mean of 70% and a 95%-CI of
404 [47%; 94%]) (Mantilla-Calderon et al., 2022). However, 92% of sewage samples showed
405 concentrations below the LOQ. By definition, the concentrations below LOQ are not
406 quantitatively reliable and may differ from the actual virus concentrations. Therefore, we

407 concluded that the unclear relationship between the WBE and the clinical epidemiological data
408 was attributed to a low number of COVID-19 cases in sewersheds and low SARS-CoV-2
409 concentrations in sewage.

410



411 **Fig 2.** Stacked histograms for (A) COVID-19 daily cases in sewersheds and (B) SARS-CoV-2
412 concentrations in sewage.
413
414

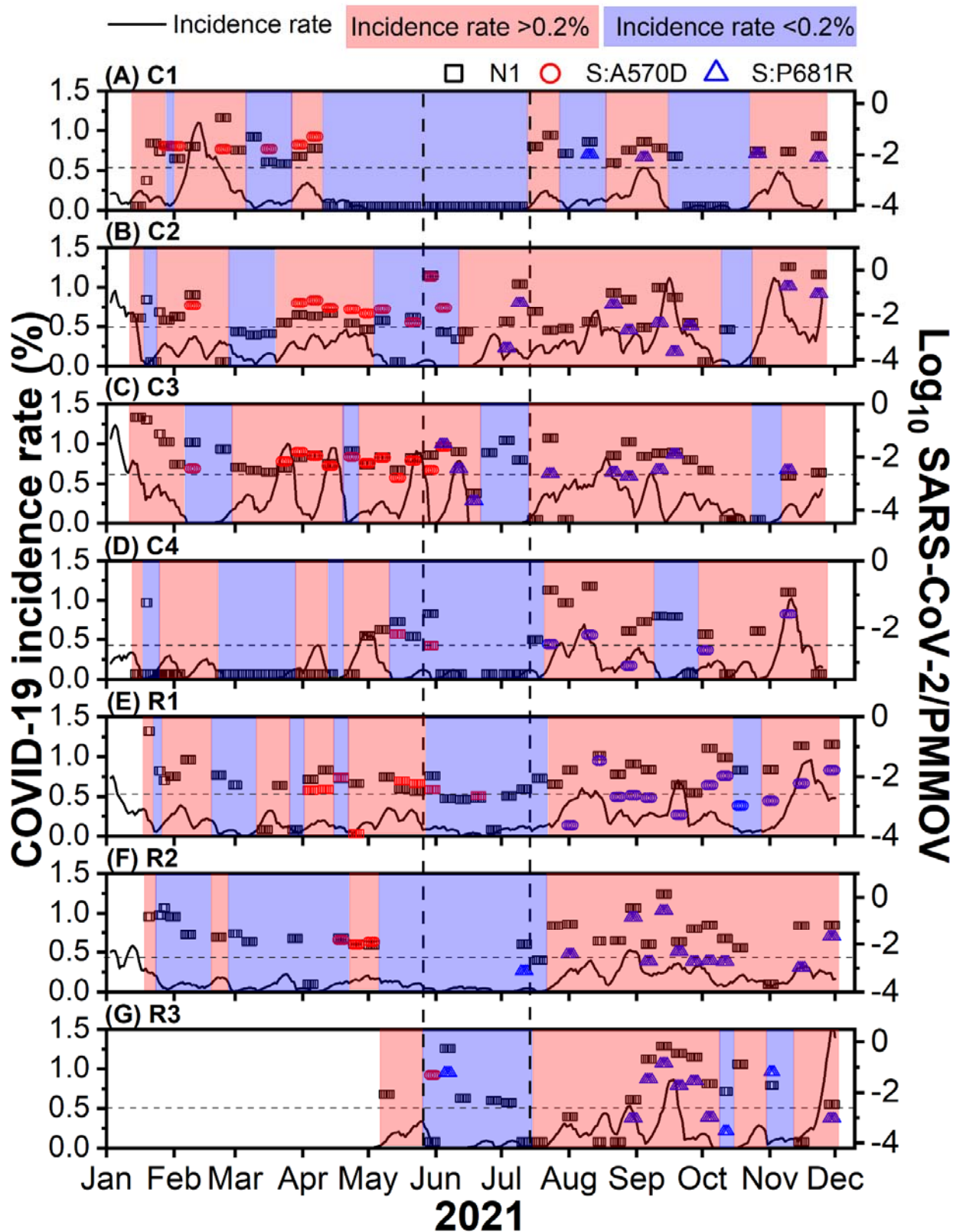
415 Application of wastewater-based epidemiology to neighborhood-scale sewersheds with low 416 COVID-19 incidence rates

417 We categorized WBE (i.e., N/PMMOV) and clinical epidemiological data (i.e., incidence rate)
418 into two groups and compared the two epidemiological data sets. Firstly, 200 or more new
419 COVID-19 cases per 100,000 populations in the past 7 days is one of the metrics that the Centers
420 for Disease Control and Prevention (CDC) uses to decide on the high-risk COVID-19
421 transmission (U.S. CDC, 2022b), which is equivalent to a 0.2% incidence rate (Eq. 9). We
422 adopted the threshold of 0.2% to categorize incidence rates into high and low levels. Monitoring
423 periods with incidence rates higher or lower than the threshold of 0.2% are shaded by red and

424 blue in **Fig. 3**. The incidence rates were higher than the threshold 158 times (i.e., high incidence
425 rate) and lower 95 times (i.e., low incidence rate) in the seven sewersheds. We investigated if
426 WBE data can estimate these high and low COVID-19 incidence periods. Thus, secondly, we
427 statistically determined a threshold of N/PMMOV, grouping them into a high or low level. The
428 ROC curve summarizes sensitivity and specificity with a series of thresholds of N/PMMOV (**Fig.**
429 **4**). We chose $10^{-2.6}$ as the unbiased optimal threshold of N/PMMOV because it gives the highest
430 geometric mean (G-mean) (Gour and Jain, 2022). The threshold of N/PMMOV is the horizontal
431 dashed line in **Fig. 3**. The N/PMMOV values were higher than the threshold 174 times and lower
432 79 times. With the threshold of $10^{-2.6}$, we can predict the COVID-19 incidence rate higher than
433 0.2% with a sensitivity of 0.82 and a specificity of 0.51. Note that there were probably
434 unreported COVID-19 cases in our sewersheds. For example, the CDC estimates that actual
435 COVID-19 infections are 6 to 24 times higher than reported cases (Havers et al., 2020). These
436 unreported COVID cases might have accounted for the false-positive scenarios where the high
437 N/PMMOV was detected from sewage samples while the COVID-19 incidence rate was low. If
438 so, the true specificity becomes higher than 0.51. These findings suggest that the threshold of
439 N/PMMOV of $10^{-2.6}$ can be used to indicate the high risk of COVID-19 transmission in the
440 neighborhood-scale sewersheds.

441

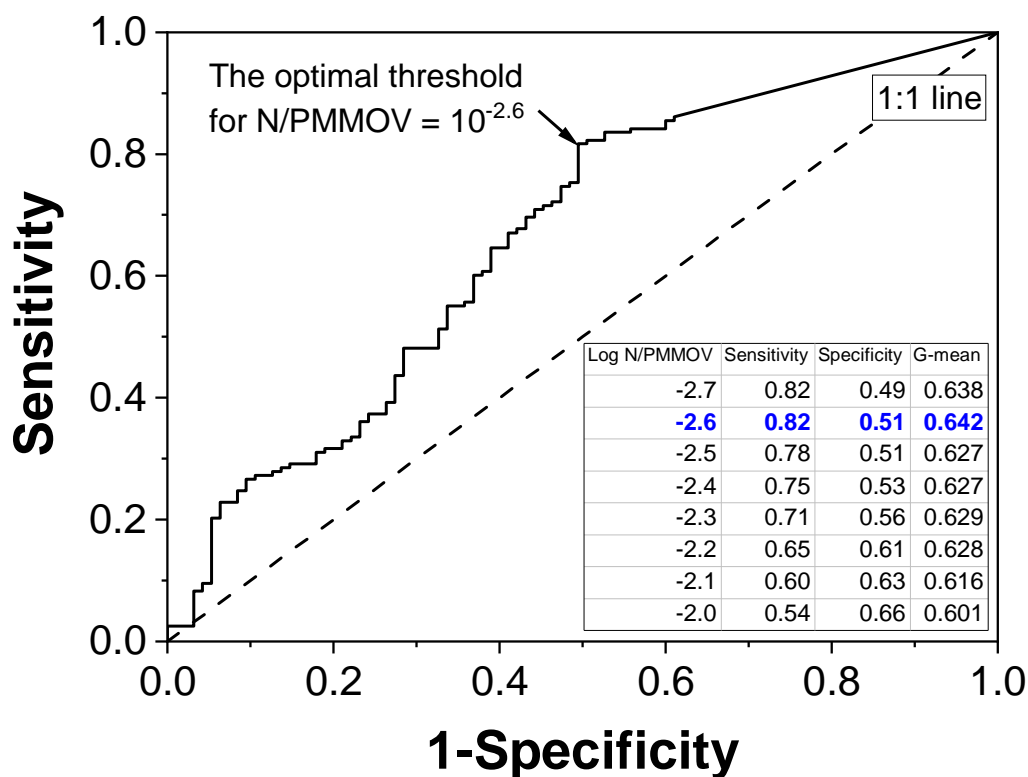
442



443
444 **Fig. 3.** Comparisons between clinical epidemiology (COVID-19 incidence rate) and wastewater-
445 based epidemiology (Log₁₀ SARS-CoV-2/PMMOV). Open symbols represent WBE results (i.e.,

446 black rectangles represent the N gene, red circles represent the S:A570D mutation (potentially
 447 indicating the Alpha variant), and blue triangles represent S:P681R (potentially representing the
 448 Delta variant). The horizontal dashed lines show the threshold N/PMMOV of $10^{-2.6}$. We assigned
 449 about 10^{-4} of N/PMMOV to samples tested negative for the N gene to differentiate these samples
 450 from samples that were not measured. Black solid curves show the COVID-19 incidence rates.
 451 The monitoring period is separated either into the high (red) or the low level (blue) with the
 452 criteria of a 0.2% incidence rate. Vertical dashed lines indicate the monitoring period from May
 453 28 to July 12 when the incidence rate on a county-scale was below 0.05%.
 454

455



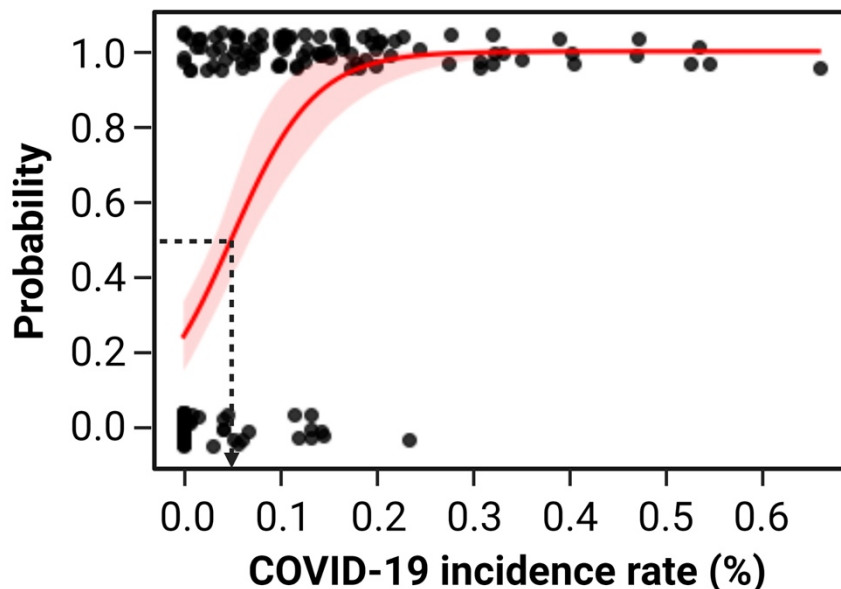
456
 457 **Fig. 4.** ROC curve with a series of N/PMMOV values when a COVID-19 incidence rate is 0.2%.
 458 The area under the curve (AUC) is 0.66 with 95% CI[0.59; 0.73]. The sensitivity and specificity
 459 with N/PMMOV of $10^{-2.6}$ are 0.82 and 0.51, respectively. The dashed line indicates a 1:1 line.
 460

461 We determined a sensitivity of our WBE procedure, defined as the COVID-19 incidence
 462 rate at which viruses in sewage are detected at 50% probability. The data from C1 was used for a
 463 binary logistic regression analysis because the COVID-19 incidence rate is most reliable in C1
 464 due to the mandatory COVID-19 testing. We found that the COVID-19 incidence rate is a

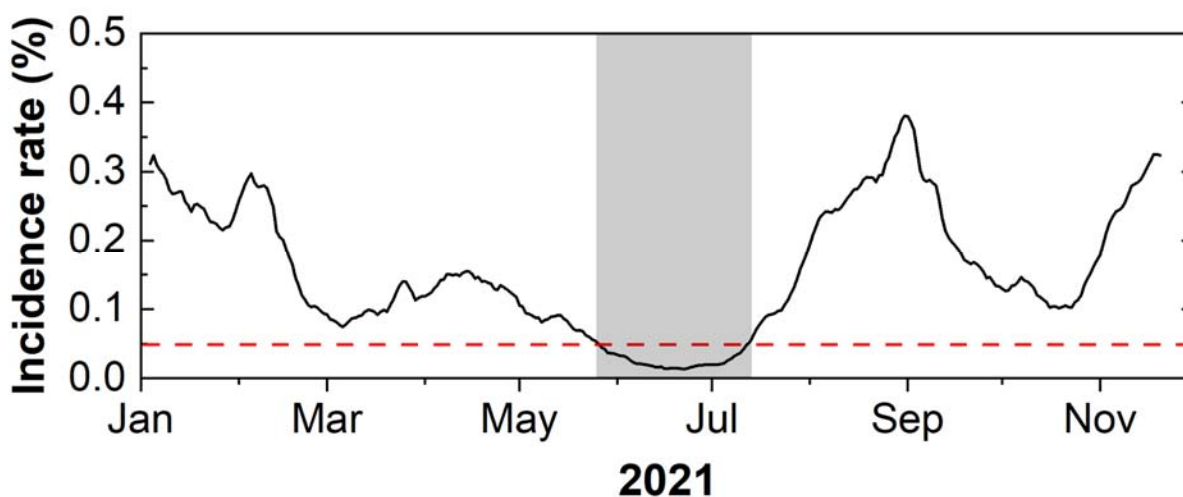
465 reliable predictor to explain the probability of SARS-CoV-2 N gene detection (McFadden;
466 $p < 0.001$). Based on the logistic regression curve in **Fig. 5**, we determined 0.05% for the WBE
467 sensitivity (or one infection case out of 2000 residents). **Fig. 6** shows the COVID-19 incidence
468 rate in Champaign County, which includes all seven sewersheds during the same monitoring
469 period as our WBE program. We found the incidence rate was less than the WBE sensitivity
470 (0.05%) from May 27 to July 12 on a county-scale, suggesting that viruses would not have been
471 detected from sewage if the WBE had been applied to the entire county during this low incidence
472 rate period.

473 However, local outbreaks with incidence rates higher than 0.2% were reported from
474 Locations C2 and C3 from May 27 to July 12 when the county-scale incidence rate was below
475 the WBE sensitivity (0.05%). These examples show that incidence rates on neighborhood-scale
476 sewersheds could be different from those on a county-scale sewershed. We found that the
477 N/PMMOV values were higher than the threshold of $10^{-2.6}$ at Locations C2 and C3, which means
478 the neighborhood-scale WBE correctly indicates these local outbreaks. More importantly, the
479 introduction of the Delta variant to Champaign County (i.e., Locations C3 and R3) was first
480 reported by our wastewater surveillance on June 6. The detection of the Delta variant by
481 neighborhood scale WBE preceded the clinical epidemiology data. Three cases of Delta variant
482 infections (GISAID ID: EPI_ISL_2885447, EPI_ISL_2885451, and EPI_ISL_2885452) were
483 first confirmed by clinical tests on June 27 and reported on July 9 in Champaign County (**Fig.**
484 **S8**). Also, these local outbreaks associated with the emerging variants would not have been
485 identified if WBE was applied to county-scale sewershed because of the incidence rate below the
486 WBE sensitivity.

487



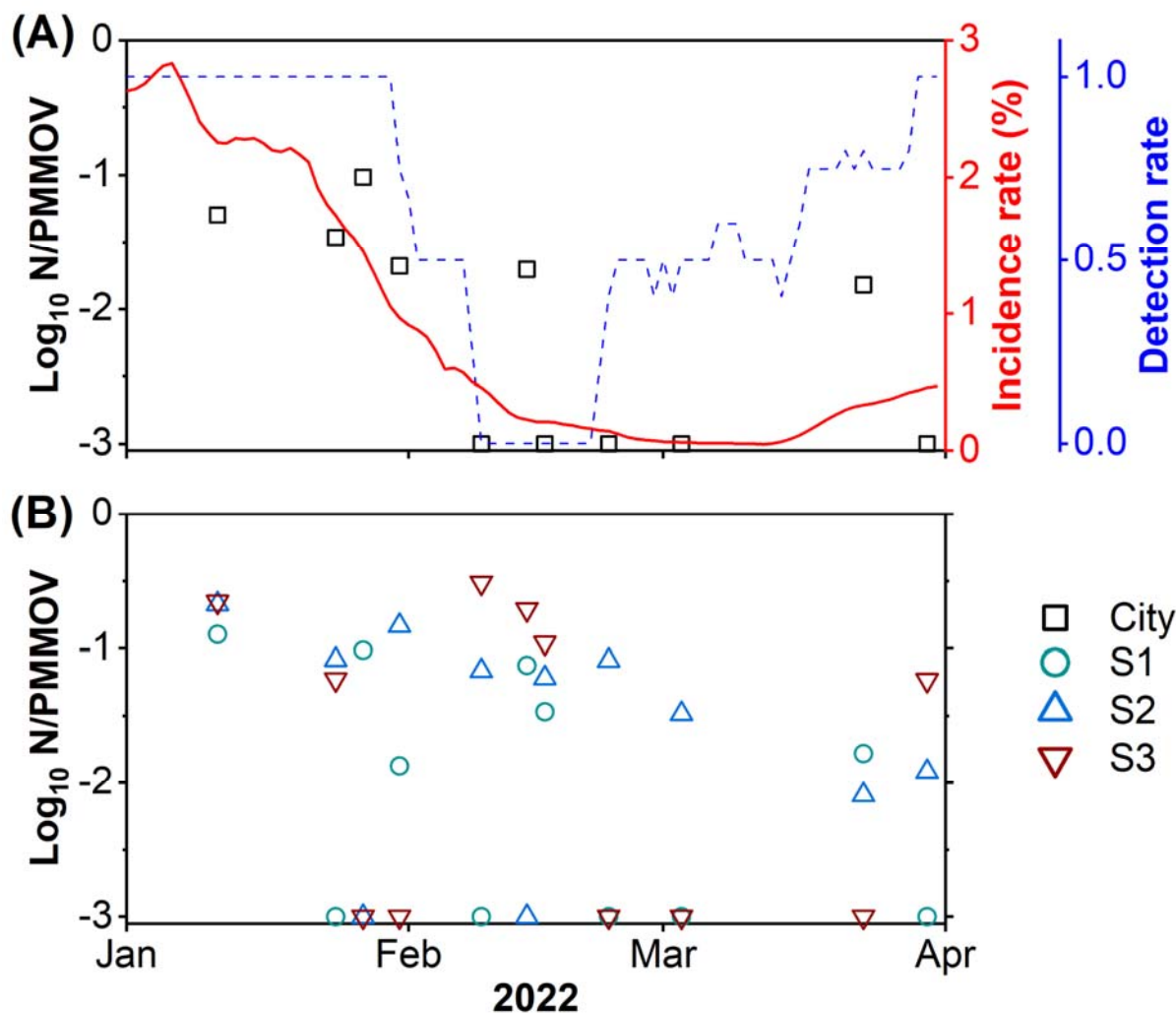
488
489 **Fig. 5.** Probability of detecting SARS-CoV-2 N gene in sewage samples from location C1. Black
490 closed-circles represent COVID-19 incidence rates on the x-axis. Either 1 or 0 was given to the
491 y-value when sewage samples tested positive or negative for SARS-CoV-2, respectively.
492 Logistic regression curves with a 95% confidence interval are represented by a red solid line and
493 shade. McFadden's Pseudo R-squared of the regression analysis was 0.34 ($p < 0.001$), which is
494 considered a good fit (McFadden, 2021). The Black dotted line indicates that the 0.05%
495 incidence rate results in a 50% probability.
496



497
498 **Fig. 6.** COVID-19 incidence rate in Champaign County. The red dashed line indicates a 0.05%
499 of incidence rate with which viruses in sewage discharged from a county-scale sewershed are
500 expected to be detected with 50% probability. The gray shade represents the monitoring period
501 showing the incidence rates lower than 0.05%.
502

503 To elucidate the effect of a sewershed size on SARS-CoV-2 N gene detection, we
504 monitored sewage samples from another set of sewersheds, including three neighborhood
505 schools (S1, S2, and S3) and one city-scale sewershed (City), from January to March 2022. This
506 monitoring period presents a decreasing tendency of incidence rate after the outbreak caused by
507 the Omicron variant. **Fig. 7A** shows WBE and clinical epidemiology data from city-scale
508 sewershed. The incidence rate decreased steadily and became lower than 1% in February 2022.
509 The detection rate of the N gene was 55% during the entire monitoring period (6 positives out of
510 11 samplings) but decreased to 29% (2 positives out of 7 samplings) in February 2022. The
511 reduction of the N gene detection rate is expected due to the low incidence rate on a city-scale.
512 The National Wastewater Surveillance System (NWSS) provides information on the detection
513 rate of SARS-CoV-2 from a wastewater treatment plant in Champaign city
514 (<https://covid.cdc.gov/covid-data-tracker/#wastewater-surveillance>; sewershed 655) (a blue
515 dashed line in **Fig. 7A**). The detection rate by NWSS agrees with our wastewater surveillance
516 program, showing a decreasing detection rate from February 2022. On the other hand, the
517 average N gene detection rate from the three smaller-scale sewersheds was stable regardless of
518 the city-scale incidence rate, showing a 64% of detection rate (21 positives out of 33 samplings)
519 during the entire period and 62% during the low incidence rate from February 2022 (13 positives
520 out of 21 samplings). Location B2 reported positives for N/PMMOV throughout the monitoring
521 period with especially a high detection rate of 82% (6 positives out of 7 samplings) when the
522 incidence rate on a city-scale was low (**Fig. 7B**). These findings corroborate that wastewater
523 surveillance should be performed at a smaller-scale sewershed to discern local outbreaks when
524 the COVID-19 incidence rate is low.

525



526
527 **Fig. 7.** COVID-19 surveillance data at (A) one city-scale sewershed and (B) three neighborhood
528 schools. A solid red line indicates the COVID-19 incidence rate from a city-scale sewershed. A
529 blue dashed line represents the detection rate of the N gene published by the National
530 Wastewater Surveillance System (NWSS).
531

532 **Implication**

533 We suggested using a threshold of N/PMMOV to indicate a high level of the COVID-19
534 incidence rate. The ROC curve (**Fig. 4**) shows that sensitivity increased from 0.54 to 0.82 while
535 the specificity decreased from 0.66 to 0.49 when N/PMMOV lowered from $10^{-2.0}$ to $10^{-2.7}$.
536 Although we selected an unbiased threshold of $10^{-2.6}$ based on the highest geometric mean,
537 different thresholds of N/PMMOV can be applied to the other sites considering regional

538 characteristics such as local public health policies and the community's acceptance of the
539 COVID-19 risk (Dryhurst et al., 2020; Turska-Kawa and Pilch, 2022). Intensive care unit (ICU)
540 occupancy rate, influenced by vulnerable populations and ICU bed capacity, may be one of the
541 regional characteristics that should be considered to determine a threshold of N/PMMOV. If
542 some regions had experienced a high ICU occupancy rate during the COVID-19 pandemic,
543 COVID-19 put enormous stress on the local medical systems. Similar scenarios could happen
544 again in the future. According to CDC, the maximum ICU occupancy rate significantly differs
545 from site to site (<http://covid.cdc.gov/covid-data-tracker>). For example, in Illinois (USA), some
546 counties, such as Cook County and Champaign County, have managed ICU beds well during the
547 COVID-19 pandemic, showing 35% of maximum ICU bed occupancy. On the other hand, other
548 counties, including Rock Island County (85%) and Effingham County (70%), experienced a
549 more significant burden on ICU beds during the COVID-19 pandemic. Therefore, these counties
550 may need to be more vigilant about the COVID-19 outbreak by setting a lower threshold.

551 Applying WBE to neighborhood-scale sewersheds may cost more than large-size
552 sewersheds for monitoring the entire administrative area. To efficiently monitor multiple
553 neighborhood-scale sewersheds, the WBE can be deployed to some representative places of
554 diverse societal characteristics, such as socioeconomic status, demographics, or land use
555 category, so that we can minimize the number of monitoring sites while obtaining information
556 about the COVID-19 incidence representative of the entire area. The COVID-19 pandemic
557 disproportionally has impacted people depending on demographic and socioeconomic status
558 (Bassett et al., 2020; Krieger, 2020). Thus, those underserved regions could be chosen for
559 wastewater surveillance. For example, we chose the nine sewersheds (Locations C2, C3, C4, R1,
560 R2, R3, S1, S2, and S3) based on areas that reported fewer cases of COVID-19 testing than the

561 average testing in Champaign County to attempt to supplement clinical testing data, while we
562 selected another sewershed to represent the highly tested campus area (location C1) (**Table S8**).
563 In addition, sample collection frequency can be optimized to operate WBE within a budget.
564 Schoen et al. (2022) found that a sampling frequency of once every 4 days is not significantly
565 different from daily sampling in estimating clinical epidemiology data. Therefore, we collected
566 4-day composite samples with a less frequent sampling frequency, once every 8.2 days.

567 We suggest that the low correlation coefficients between WBE and the clinical data can
568 be explained by the fact that heterogeneity of clinical symptoms becomes significant with a low
569 COVID-19 incidence rate in neighborhood-scale sewersheds. However, these correlation
570 coefficients may become higher if our wastewater surveillance protocol is more sensitive to
571 detecting the N gene from sewage samples. Although the median of our LODs was $3.78 \log_{10}$
572 gc/L , which is within the reasonable range compared to other studies ($3.0 \log_{10} \text{gc/L}$ (10th
573 percentile) to $6.1 \log_{10} \text{gc/L}$ (90th percentile) (Pecson et al., 2021), the WBE sensitivity could be
574 getting better as WBE is getting matured. Then, the correlation coefficients could be higher, and
575 it could be possible to quantitatively estimate the COVID-19 incidence rate with N/PMMOV.

576 Our findings on the neighborhood-scale WBE have significant implications for public
577 health. COVID-19 might be moving from a pandemic to an endemic phase (Veldhoen and Pedro
578 Simas, 2021), which involves a difference in disease surveillance strategy. In an endemic phase,
579 we may not be able to get as accurate statistics on COVID-19 by the clinical diagnosis as we did
580 in the pandemic phase because people will be less likely to visit hospitals to get tested or medical
581 support. This is because the illnesses may be self-limiting (Veldhoen and Pedro Simas, 2021).
582 People also may have less accessibility to testing sites and use rapid COVID-19 test kits at home
583 (Kost, 2022). In this context, WBE will play a pivotal role in the COVID-19 surveillance

584 because WBE provides unbiased information about all residents in the sewershed. Lak et al.
585 (2021) and Shi et al. (2021) discovered that local COVID-19 outbreaks could spread through the
586 surrounding regions resulting in other outbreaks. Rader et al. (2020) explained the fast virus
587 transmission to the surrounding areas with frequent contact among residents. These studies
588 highlight the necessity of early detection of local COVID-19 outbreaks (Cariti et al., 2022; Wu et
589 al., 2022a). Our study shows that WBE should be applied to neighborhood-scale sewershed to
590 identify covert local outbreaks in advance and the introduction of emerging SARS-CoV-2
591 variants, which provides a warning for large-scale outbreaks.

592

593 **Conclusion**

594 In this study, we applied WBE to seven neighborhood-scale sewersheds (an average catchment
595 population was 1471) for eleven months. We found that WBE data from neighborhood-scale
596 sewersheds were poorly correlated to clinical testing data when COVID-19 incidence was low.
597 Thus, we suggest a threshold of N/PMMOV to indicate a high level of COVID-19 incidence
598 rates, which can be assigned in collaboration with public health officials. We demonstrated that
599 this approach could discern local COVID-19 outbreaks that a county-scale WBE would not
600 detect due to the low disease incidence on a county scale. Our findings highlight that WBE
601 should be applied to neighborhood-scale sewersheds when COVID-19 incidence is maintained at
602 a low level.

603

604 **Acknowledgment**

605 We acknowledge the funding from the Grainger College of Engineering, the JUMP-ARCHES
606 program of OSF Healthcare in conjunction with the University of Illinois, and the VinUni

607 Illinois Smart Health Center. We thank Brad Bennett and Bruce Rabe at the Urbana-Champaign
608 Sanitary District and Haley Turner and Travis Ramme at the Rantoul Wastewater Treatment
609 Plant for providing us with influent wastewater. The authors also acknowledge Kip Stevenson
610 for sampling deployment, and Yuqing Mao, Matthew Robert Loula, Aashna Patra, Kristin Joy
611 Anderson, Mikayla Diedrick, Hubert Lyu, Hamza Elmahi Mohamed, Jad R Karajeh, Runsen
612 Ning, Rui Fu, and Kyukyong Kim for sewage sampling and processing. We also acknowledge
613 Dr. Awais Vaid for guidance on sampling site selection.

614

615

616

617 **References**

- 618 Abrams, E.M., Szeffler, S.J., 2020. COVID-19 and the impact of social determinants of health.
619 *Lancet Respir. Med.* 8, 659–661.
- 620 Ahmed, W., Bertsch, P.M., Bibby, K., Haramoto, E., Hewitt, J., Huygens, F., Gyawali, P.,
621 Korajkic, A., Riddell, S., Sherchan, S.P., Simpson, S.L., Sirikanjana, K., Symonds, E.M.,
622 Verhagen, R., Vasan, S.S., Kitajima, M., Bivins, A., 2020a. Decay of SARS-CoV-2 and
623 surrogate murine hepatitis virus RNA in untreated wastewater to inform application in
624 wastewater-based epidemiology. *Environ. Res.* 191, 110092.
- 625 Ahmed, W., Bertsch, P.M., Bivins, A., Bibby, K., Farkas, K., Gathercole, A., Haramoto, E.,
626 Gyawali, P., Korajkic, A., McMinn, B.R., Mueller, J.F., Simpson, S.L., Smith, W.J.M.,
627 Symonds, E.M., Thomas, K. V., Verhagen, R., Kitajima, M., 2020b. Comparison of virus
628 concentration methods for the RT-qPCR-based recovery of murine hepatitis virus, a
629 surrogate for SARS-CoV-2 from untreated wastewater. *Sci. Total Environ.* 739, 139960.
- 630 Barrios, R.E., Lim, C., Kelley, M.S., Li, X., 2021. SARS-CoV-2 concentrations in a wastewater
631 collection system indicated potential COVID-19 hotspots at the zip code level. *Sci. Total*
632 *Environ.* 800, 149480.
- 633 Barua, V.B., Juel, M.A.I., Blackwood, A.D., Clerkin, T., Ciesielski, M., Sorinolu, A.J., Holcomb,
634 D.A., Young, I., Kimble, G., Sypolt, S., Engel, L.S., Noble, R.T., Munir, M., 2022.
635 Tracking the temporal variation of COVID-19 surges through wastewater-based
636 epidemiology during the peak of the pandemic: A six-month long study in Charlotte, North
637 Carolina. *Sci. Total Environ.* 814, 152503.
- 638 Bassett, M.T., Chen, J.T., Krieger, N., 2020. Variation in racial/ethnic disparities in COVID-19
639 mortality by age in the United States: A cross-sectional study. *PLOS Med.* 17, e1003402.

- 640 Bitter, L.C., Kibbee, R., Jiménez, G.C., Rmeci, B.O. □, 2022. Wastewater Surveillance of SARS-
641 CoV-2 at a Canadian University Campus and the Impact of Wastewater Characteristics on
642 Viral RNA Detection. ACS ES&T Water.
643 <https://doi.org/10.1021/ACSESTWATER.2C00060>.
- 644 Bivins, A., Bibby, K., 2021. Wastewater Surveillance during Mass COVID-19 Vaccination on a
645 College Campus. Environ. Sci. Technol. Lett. 8, 792–798.
- 646 Bustin, S.A., Benes, V., Garson, J.A., Hellemans, J., Huggett, J., Kubista, M., Mueller, R., Nolan,
647 T., Pfaffl, M.W., Shipley, G.L., Vandesompele, J., Wittwer, C.T., 2009. The MIQE
648 guidelines: Minimum information for publication of quantitative real-time PCR experiments.
649 Clin. Chem. 55, 611–622.
- 650 Cariti, F., Tuñ As Corzon, A., Fernandez-Cassi, X., Ganesanandamoorthy, P., Ort, C., Julian,
651 T.R., Kohn, T., 2022. Wastewater Reveals the Spatiotemporal Spread of SARS-CoV-2 in
652 the Canton of Ticino (Switzerland) during the Onset of the COVID-19 Pandemic. ACS
653 ES&T Water. <https://doi.org/10.1021/ACSESTWATER.2C00082>
- 654 Castro-Gutierrez, V., Hassard, F.I., Vu, M.I., Leitao, R., Burczynska, B., WildeboerID, D.,
655 Stanton, I., Rahimzadeh, S., Baio, G., GarelickID, H., HofmanID, J., Kasprzyk-Hordern, B.,
656 KwiatkowskaID, R., Majeed, A., Priest, S., Grimsley, J., Lundy, L., SingerID, A.C., Di
657 CesareID, M., 2022. Monitoring occurrence of SARS-CoV-2 in school populations: A
658 wastewater-based approach. PLoS One 17, e0270168.
- 659 Catherine Hoar, Francoise Chauvin, Alexander Clare, Hope McGibbon, Esmeraldo Castro,
660 Samantha Patinella, Dimitrios Katehis, J. Dennehy, J., Monica Trujillo, S. Smyth, D.,
661 I. Silverman, A., 2022. Monitoring SARS-CoV-2 in wastewater during New York City's
662 second wave of COVID-19: sewershed-level trends and relationships to publicly available

663 clinical testing data. *Environ. Sci. Water Res. Technol.* 8, 1021–1035.

664 Chen, Y., Chen, L., Deng, Q., Zhang, G., Wu, K., Ni, L., Yang, Y., Liu, B., Wang, W., Wei, C.,
665 Yang, J., Ye, G., Cheng, Z., 2020. The presence of SARS-CoV-2 RNA in the feces of
666 COVID-19 patients. *J. Med. Virol.* 92, 833–840.

667 D’Aoust, P.M., Mercier, E., Montpetit, D., Jia, J.J., Alexandrov, I., Neault, N., Baig, A.T.,
668 Mayne, J., Zhang, X., Alain, T., Langlois, M.A., Servos, M.R., MacKenzie, M., Figeys, D.,
669 MacKenzie, A.E., Graber, T.E., Delatolla, R., 2021. Quantitative analysis of SARS-CoV-2
670 RNA from wastewater solids in communities with low COVID-19 incidence and prevalence.
671 *Water Res.* 188, 116560.

672 Dryhurst, S., Schneider, C.R., Kerr, J., Freeman, A.L.J., Recchia, G., van der Bles, A.M.,
673 Spiegelhalter, D., van der Linden, S., 2020. Risk perceptions of COVID-19 around the
674 world. *J. Risk Res.* 23, 994–1006.

675 Feng, S., Roguet, A., McClary-Gutierrez, J.S., Newton, R.J., Kloczko, N., Meiman, J.G.,
676 McLellan, S.L., 2021. Evaluation of Sampling, Analysis, and Normalization Methods for
677 SARS-CoV-2 Concentrations in Wastewater to Assess COVID-19 Burdens in Wisconsin
678 Communities. *ACS ES&T Water* 1, 1955–1965.

679 Fitzgerald, S.F., Rossi, G., Low, A.S., McAteer, S.P., O’Keefe, B., Findlay, D., Cameron, G.J.,
680 Pollard, P., Singleton, P.T.R., Ponton, G., Singer, A.C., Farkas, K., Jones, D., Graham,
681 D.W., Quintela-Baluja, M., Tait-Burkard, C., Gally, D.L., Kao, R., Corbishley, A., 2021.
682 Site Specific Relationships between COVID-19 Cases and SARS-CoV-2 Viral Load in
683 Wastewater Treatment Plant Influent. *Environ. Sci. Technol.* 55, 15276–15286.

684 Gibas, C., Lambirth, K., Mittal, N., Juel, M.A.I., Barua, V.B., Roppolo Brazell, L., Hinton, K.,
685 Lontai, J., Stark, N., Young, I., Quach, C., Russ, M., Kauer, J., Nicolosi, B., Chen, D.,

- 686 Akella, S., Tang, W., Schlueter, J., Munir, M., 2021. Implementing building-level SARS-
687 CoV-2 wastewater surveillance on a university campus. *Sci. Total Environ.* 782, 146749.
- 688 Gour, M., Jain, S., 2022. Automated COVID-19 detection from X-ray and CT images with
689 stacked ensemble convolutional neural network. *Biocybern. Biomed. Eng.* 42, 27–41.
- 690 Hart, O.E., Halden, R.U., 2020. Computational analysis of SARS-CoV-2/COVID-19
691 surveillance by wastewater-based epidemiology locally and globally: Feasibility, economy,
692 opportunities and challenges. *Sci. Total Environ.* 730, 138875.
- 693 Hata, A., Hara-Yamamura, H., Meuchi, Y., Imai, S., Honda, R., 2021. Detection of SARS-CoV-
694 2 in wastewater in Japan during a COVID-19 outbreak. *Sci. Total Environ.* 758, 143578.
- 695 Havers, F.P., Reed, C., Lim, T., Montgomery, J.M., Klena, J.D., Hall, A.J., Fry, A.M., Cannon,
696 D.L., Chiang, C.F., Gibbons, A., Krapinunaya, I., Morales-Betoulle, M., Roguski, K.,
697 Rasheed, M.A.U., Freeman, B., Lester, S., Mills, L., Carroll, D.S., Owen, S.M., Johnson,
698 J.A., Semenova, V., Blackmore, C., Blog, D., Chai, S.J., Dunn, A., Hand, J., Jain, S.,
699 Lindquist, S., Lynfield, R., Pritchard, S., Sokol, T., Sosa, L., Turabelidze, G., Watkins, S.M.,
700 Wiesman, J., Williams, R.W., Yendell, S., Schiffer, J., Thornburg, N.J., 2020.
701 Seroprevalence of Antibodies to SARS-CoV-2 in 10 Sites in the United States, March 23-
702 May 12, 2020. *JAMA Intern. Med.* 180, 1576–1586.
- 703 He, X., Lau, E.H.Y., Wu, P., Deng, X., Wang, J., Hao, X., Lau, Y.C., Wong, J.Y., Guan, Y., Tan,
704 X., Mo, X., Chen, Y., Liao, B., Chen, W., Hu, F., Zhang, Q., Zhong, M., Wu, Y., Zhao, L.,
705 Zhang, F., Cowling, B.J., Li, F., Leung, G.M., 2020. Temporal dynamics in viral shedding
706 and transmissibility of COVID-19. *Nat. Med.* 2020 265 26, 672–675.
- 707 Hewitt, J., Trowsdale, S., Armstrong, B.A., Chapman, J.R., Carter, K.M., Croucher, D.M., Trent,
708 C.R., Sim, R.E., Gilpin, B.J., 2022. Sensitivity of wastewater-based epidemiology for

709 detection of SARS-CoV-2 RNA in a low prevalence setting. *Water Res.* 211, 118032.

710 Jamal, Y., Gangwar, M., Usmani, M., Adams, A., Wu, C.-Y., Nguyen, T.H., Colwell, R., Jutla,
711 A., 2022. Identification of thresholds on population density for understanding transmission
712 of COVID-19. *GeoHealth* e2021GH000449.

713 Karthikeyan, S., Nguyen, A., McDonald, D., Zong, Y., Ronquillo, N., Ren, J., Zou, J., Farmer, S.,
714 Humphrey, G., Henderson, D., Javidi, T., Messer, K., Anderson, C., Schooley, R., Martin,
715 N.K., Knight, R., 2021. Rapid, Large-Scale Wastewater Surveillance and Automated
716 Reporting System Enable Early Detection of Nearly 85% of COVID-19 Cases on a
717 University Campus. *mSystems* 6.

718 Ke, R., Martinez, P.P., Smith, R.L., Gibson, L.L., Mirza, A., Conte, M., Gallagher, N., Luo, C.H.,
719 Jarrett, J., Zhou, R., Conte, A., Liu, T., Farjo, M., Walden, K.K.O., Rendon, G., Fields, C.J.,
720 Wang, L., Fredrickson, R., Edmonson, D.C., Baughman, M.E., Chiu, K.K., Choi, H.,
721 Scardina, K.R., Bradley, S., Gloss, S.L., Reinhart, C., Yedetore, J., Quicksall, J., Owens,
722 A.N., Broach, J., Barton, B., Lazar, P., Heetderks, W.J., Robinson, M.L., Mostafa, H.H.,
723 Manabe, Y.C., Pekosz, A., McManus, D.D., Brooke, C.B., 2022. Daily longitudinal
724 sampling of SARS-CoV-2 infection reveals substantial heterogeneity in infectiousness. *Nat.*
725 *Microbiol.* 2022 75 7, 640–652.

726 Kost, G.J., 2022. Diagnostic Strategies for Endemic Coronavirus Disease 2019 (COVID-
727 19)Rapid Antigen Tests, Repeated Testing, and Prevalence Boundaries. *Arch. Pathol. Lab.*
728 *Med.* 146, 16–25.

729 Krieger, N., 2020. ENOUGH: COVID-19, structural racism, police brutality, plutocracy, climate
730 change-and time for health justice, democratic governance, and an equitable, sustainable
731 future. *Am. J. Public Health* 110, 1620–1623.

- 732 Lak, A., Sharifi, A., Badr, S., Zali, A., Maher, A., Mostafavi, E., Khalili, D., 2021. Spatio-
733 temporal patterns of the COVID-19 pandemic, and place-based influential factors at the
734 neighborhood scale in Tehran. *Sustain. Cities Soc.* 72, 103034.
- 735 Li, X., Kulandaivelu, J., Zhang, S., Shi, J., Sivakumar, M., Mueller, J., Luby, S., Ahmed, W.,
736 Coin, L., Jiang, G., 2021. Data-driven estimation of COVID-19 community prevalence
737 through wastewater-based epidemiology. *Sci. Total Environ.* 789, 147947.
- 738 Mantilla-Calderon, D., Huang, K., Li, A., Chibwe, K., Yu, X., Ye, Y., Liu, L., Ling, F., 2022.
739 Emerging investigator series: meta-analyses on SARS-CoV-2 viral RNA levels in
740 wastewater and their correlations to epidemiological indicators. *Environ. Sci. Water Res.*
741 *Technol.* 8, 1391–1407.
- 742 McFadden, D., 2021. Quantitative Methods for Analysing Travel Behaviour of Individuals□:
743 Some Recent Developments. *Behav. Travel Model.* 279–318.
- 744 Messner, W., Payson, S.E., 2020. Variation in COVID-19 outbreaks at the US state and county
745 levels. *Public Health* 187, 15–18.
- 746 Oh, C., Kim, K., Araud, E., Wang, L., Shisler, J.L., Nguyen, T.H., 2022a. A novel approach to
747 concentrate human and animal viruses from wastewater using receptors-conjugated
748 magnetic beads. *Water Res.* 212, 118112.
- 749 Oh, C., Sashittal, P., Zhou, A., Wang, L., El-Kebir, M., Nguyen, T.H., 2022b. Design of SARS-
750 CoV-2 Variant-Specific PCR Assays Considering Regional and Temporal Characteristics.
751 *Appl. Environ. Microbiol.* 88.
- 752 Pecson, B.M., Darby, E., Haas, C.N., Amha, Y.M., Bartolo, M., Danielson, R., Dearborn, Y., Di
753 Giovanni, G., Ferguson, C., Fevig, S., Gaddis, E., Gray, D., Lukasik, G., Mull, B., Olivas,
754 L., Olivieri, A., Qu, Y., SARS-CoV-2 Interlaboratory Consortium, 2021. Reproducibility

755 and sensitivity of 36 methods to quantify the SARS-CoV-2 genetic signal in raw wastewater:
756 findings from an interlaboratory methods evaluation in the U.S. *Environ. Sci. Water Res.*
757 *Technol.* <https://doi.org/10.1039/d0ew00946f>

758 Rački, N., Dreo, T., Gutierrez-Aguirre, I., Blejec, A., Ravnikar, M., 2014. Reverse transcriptase
759 droplet digital PCR shows high resilience to PCR inhibitors from plant, soil and water
760 samples. *Plant Methods* 2014 101 10, 1–10.

761 Rader, B., Scarpino, S. V., Nande, A., Hill, A.L., Adlam, B., Reiner, R.C., Pigott, D.M.,
762 Gutierrez, B., Zarebski, A.E., Shrestha, M., Brownstein, J.S., Castro, M.C., Dye, C., Tian,
763 H., Pybus, O.G., Kraemer, M.U.G., 2020. Crowding and the shape of COVID-19 epidemics.
764 *Nat. Med.* 2020 2612 26, 1829–1834.

765 Roldan-Hernandez, L., Graham, K.E., Duong, D., Boehm, A.B., 2022. Persistence of
766 Endogenous SARS-CoV-2 and Pepper Mild Mottle Virus RNA in Wastewater-Settled
767 Solids. *ACS Environ. Sci. Technol. Water.*
768 <https://doi.org/10.1021/ACSESTWATER.2C00003>

769 Rusiñol, M., Zammit, I., Itarte, M., Forés, E., Martínez-Puchol, S., Girones, R., Borrego, C.,
770 Corominas, L., Bofill-Mas, S., 2021. Monitoring waves of the COVID-19 pandemic:
771 Inferences from WWTPs of different sizes. *Sci. Total Environ.* 787, 147463.

772 Safford, H., Zuniga-Montanez, R.E., Kim, M., Wu, X., Wei, L., Sharpnack, J., Shapiro, K.,
773 Bischel, H.N., 2022. Wastewater-Based Epidemiology for COVID-19: Handling qPCR
774 Nondetects and Comparing Spatially Granular Wastewater and Clinical Data Trends. *ACS*
775 *ES&T Water.* <https://doi.org/10.1021/ACSESTWATER.2C00053>

776 Sangsanont, J., Rattanakul, S., Kongprajug, A., Chyerochana, N., Sresung, M., Sriporatana, N.,
777 Wanlapakorn, N., Poovorawan, Y., Mongkolsuk, S., Sirikanchana, K., 2022. SARS-CoV-2

778 RNA surveillance in large to small centralized wastewater treatment plants preceding the
779 third COVID-19 resurgence in Bangkok, Thailand. *Sci. Total Environ.* 809, 151169.

780 Schoen, M.E., Wolfe, M.K., Li, L., Duong, D., White, B.J., Hughes, B., Boehm, A.B., 2022.
781 SARS-CoV-2 RNA Wastewater Settled Solids Surveillance Frequency and Impact on
782 Predicted COVID-19 Incidence Using a Distributed Lag Model. *ACS ES&T Water.*
783 <https://doi.org/10.1021/ACSESTWATER.2C00074>

784 Seabold, S., Josef Perktold, 2010. *Statsmodels: Econometric and statistical modeling with python*,
785 in: *Proceedings of the 9th Python in Science Conference*. pp. 92–96.

786 Sherchan, S.P., Shahin, S., Patel, J., Ward, L.M., Tandukar, S., Uprety, S., Schmitz, B.W.,
787 Ahmed, W., Simpson, S., Gyawali, P., 2021. Occurrence of SARS-CoV-2 RNA in Six
788 Municipal Wastewater Treatment Plants at the Early Stage of COVID-19 Pandemic in The
789 United States. *Pathog. (Basel, Switzerland)* 10.

790 Shi, J., Gao, X., Xue, S., Li, F., Nie, Q., Lv, Y., Wang, J., Xu, T., Du, G., Li, G., 2021. Spatio-
791 temporal evolution and influencing mechanism of the COVID-19 epidemic in Shandong
792 province, China. *Sci. Reports* 2021 11, 1–16.

793 Simpson, A., Topol, A., White, B.J., Wolfe, M.K., Wigginton, K.R., Boehm, A.B., 2021. Effect
794 of storage conditions on SARS- CoV-2 RNA quantification in wastewater solids. *PeerJ* 9,
795 e11933.

796 Spurbeck, R.R., Minard-Smith, A., Catlin, L., 2021. Feasibility of neighborhood and building
797 scale wastewater-based genomic epidemiology for pathogen surveillance. *Sci. Total*
798 *Environ.* 789, 147829.

799 Tiwari, A., Phan, N., Tandukar, S., Ashoori, R., Thakali, O., Mousazadesh, M., Dehghani, M.H.,
800 Sherchan, S.P., 2021. Persistence and occurrence of SARS-CoV-2 in water and wastewater

801 environments: a review of the current literature. *Environ. Sci. Pollut. Res.* 1, 1–11.

802 Turska-Kawa, A., Pilch, I., 2022. Political beliefs and the acceptance of the SARS-CoV-2
803 pandemic restrictions. The case of Poland. *PLoS One* 17, e0264502.

804 U.S. CDC, 2022a. Wastewater Surveillance Testing Methods. URL
805 [https://www.cdc.gov/healthywater/surveillance/wastewater-surveillance/testing-](https://www.cdc.gov/healthywater/surveillance/wastewater-surveillance/testing-methods.html)
806 [methods.html](https://www.cdc.gov/healthywater/surveillance/wastewater-surveillance/testing-methods.html) (accessed 8.6.22).

807 U.S. CDC, 2022b. COVID-19 Community Levels. URL [https://www.cdc.gov/coronavirus/2019-](https://www.cdc.gov/coronavirus/2019-ncov/science/community-levels.html)
808 [ncov/science/community-levels.html](https://www.cdc.gov/coronavirus/2019-ncov/science/community-levels.html) (accessed 8.6.22).

809 Upshaw, T.L., Brown, C., Smith, R., Perri, M., Ziegler, C., Pinto, A.D., 2021. Social
810 determinants of COVID-19 incidence and outcomes: A rapid review. *PLoS One* 16,
811 e0248336.

812 Veldhoen, M., Pedro Simas, J., 2021. Covid-19 will become endemic but with decreased potency
813 over time, scientists believe. *BMJ* 372, n494.

814 Wolfe, M.K., Archana, A., Catoe, D., Coffman, M.M., Dorevich, S., Graham, K.E., Kim, S.,
815 Grijalva, L.M., Roldan-Hernandez, L., Silverman, A.I., Sinnott-Armstrong, N., Vugia, D.J.,
816 Yu, A.T., Zambrana, W., Wigginton, K.R., Boehm, A.B., 2021. Scaling of SARS-CoV-2
817 RNA in settled solids from multiple wastewater treatment plants to compare incidence rates
818 of laboratory-confirmed COVID-19 in their sewersheds. *Environ. Sci. Technol. Lett.* 8,
819 398–404.

820 Wu, F., Lee, W.L., Chen, H., Gu, X., Chandra, F., Armas, F., Xiao, A., Leifels, M., Rhode, S.F.,
821 Wuertz, S., Thompson, J., Alm, E.J., 2022a. Making waves: Wastewater surveillance of
822 SARS-CoV-2 in an endemic future. *Water Res.* 219, 118535.

823 Wu, F., Xiao, A., Zhang, J., Moniz, K., Endo, N., Armas, F., Bonneau, R., Brown, M.A.,

824 Bushman, M., Chai, P.R., Duvallet, C., Erickson, T.B., Foppe, K., Ghaeli, N., Gu, X.,
825 Hanage, W.P., Huang, K.H., Lee, W.L., Matus, M., McElroy, K.A., Nagler, J., Rhode, S.F.,
826 Santillana, M., Tucker, J.A., Wuertz, S., Zhao, S., Thompson, J., Alm, E.J., 2022b. SARS-
827 CoV-2 RNA concentrations in wastewater foreshadow dynamics and clinical presentation
828 of new COVID-19 cases. *Sci. Total Environ.* 805, 150121.

829 Wu, F., Xiao, A., Zhang, J., Moniz, K., Endo, N., Armas, F., Bushman, M., Chai, P.R., Duvallet,
830 C., Erickson, T.B., Foppe, K., Ghaeli, N., Gu, X., Hanage, W.P., Huang, K.H., Lee, W.L.,
831 McElroy, K.A., Rhode, S.F., Matus, M., Wuertz, S., Thompson, J., Alm, E.J., 2021.
832 Wastewater surveillance of SARS-CoV-2 across 40 U.S. states from February to June 2020.
833 *Water Res.* 202, 117400.

834 Xiao, A., Wu, F., Bushman, M., Zhang, J., Imakaev, M., Chai, P.R., Duvallet, C., Endo, N.,
835 Erickson, T.B., Armas, F., Arnold, B., Chen, H., Chandra, F., Ghaeli, N., Gu, X., Hanage,
836 W.P., Lee, W.L., Matus, M., McElroy, K.A., Moniz, K., Rhode, S.F., Thompson, J., Alm,
837 E.J., 2022. Metrics to relate COVID-19 wastewater data to clinical testing dynamics. *Water*
838 *Res.* 212, 118070.

839 Zhan, Q., Babler, K.M., Sharkey, M.E., Amirali, A., Beaver, C.C., Boone, M.M., Comerford, S.,
840 Cooper, D., Cortizas, E.M., Currall, B.B., Fook, J., Grills, G.S., Kobetz, E., Kumar, N.,
841 Laine, J., Lamar, W.E., Mantero, A.M.A., Mason, C.E., Reding, B.D., Robertson, M., Roca,
842 M.A., Ryon, K., Schürer, S.C., Shukla, B.S., Solle, N.S., Stevenson, M., Jr, J.J.T., Thomas,
843 C., Thomas, T., Vidović, D., Williams, S.L., Yin, X., Solo-Gabriele, H.M., 2022.
844 Relationships between SARS-CoV-2 in Wastewater and COVID-19 Clinical Cases and
845 Hospitalizations, with and without Normalization against Indicators of Human Waste. *ACS*
846 *ES&T Water.* <https://doi.org/10.1021/ACSESTWATER.2C00045>

847

848